Mixing of dense fluid in a turbulent pipe flow

Part 2. Dependence of transfer coefficients on local stability

By T. H. ELLISON AND J. S. TURNER
Department of the Mechanics of Fluids, University of Manchester

(Received 5 January 1960)

This paper continues an investigation into the mixing of a dense layer of salt solution in a turbulent pipe flow in order to obtain a more detailed understanding of the underlying physical processes. The effect of the density difference on the velocity profile in a sloping pipe is calculated using a simplified model, and the results compared with direct measurements obtained by timing streaks of dye at various levels in the pipe. These velocity profiles are also used in conjunction with density profiles to estimate the dependence of the transfer coefficients for salt and momentum, K_S and K_M, on stability.

It is found that K_S is much more greatly affected by the density gradient than K_M, and that the ratio K_S/K_M may be represented, to the accuracy of the experiments, as a function of the local Richardson Number Ri. The results agree with what is known of K_S/K_M in neutral and very stable conditions, and they confirm an earlier prediction by Ellison that the critical flux Richardson number, at which K_S becomes zero, is much less than unity.

Finally, a crude semi-empirical method is outlined which indicates how the new measurements of the transfer coefficients may be related to the overall properties of the flow discussed in the first part of the paper.

1. Introduction

The first part of this paper (Ellison & Turner 1960) presented the results of measurements of the mixing of dense fluid in a turbulent stream in terms of density profiles alone. Although this is adequate for the application of the results, and may indeed be more directly useful than a more fundamental approach, a real understanding of the underlying physical phenomena can only be achieved by studying the mechanism of the flow in more detail. As the next step, this paper discusses the flow using concepts which also require a knowledge of the velocity gradients and the manner in which they are changed by the presence of a dense layer in the pipe. Simultaneous measurements of velocity and density profiles are recorded, and those for occasions when the condition of the flow was especially simple are analysed to give the turbulent transfer coefficients for salt and momentum, K_S and K_M, in terms of the local Richardson number.

2. The velocity profile

The density gradients can affect the velocity in several ways. In a tilted pipe with the flow uphill, even if K_M is not affected directly, the component of the weight of a layer of heavy fluid along the pipe will reduce the velocity near the floor and increase it near the roof. This distortion will itself lead to a change in the stress distribution and hence lead to a change in K_M, although the effect may not be great. Thirdly, there is the direct stabilizing effect of the density gradient which may modify the relation between K_M and the stress distribution. Since the heavy fluid spreads as it becomes mixed, the magnitudes of these effects change with distance producing accelerations which further complicate the flow.

It is difficult to separate the various modes of action of the density gradient experimentally, but for a given density profile the first, which depends solely on the weight of the layer, can be calculated. After setting down the equations of motion in full for future reference, we shall describe such a calculation and consider how far it explains the observed velocity profiles.

Equations of motion

Let the x-axis be along the pipe which slopes upwards at an angle α, and the z-axis across the pipe perpendicular to its floor. Then on the usual assumption that the variation of density may be neglected in the inertia terms, the x-component of the equations of motion may be written as

$$U\frac{\partial U}{\partial x}+W\frac{\partial U}{\partial z}+\frac{\partial p}{\partial x}+\Delta\sin\alpha-\frac{\partial}{\partial z}\left[(K_M+\nu)\frac{\partial U}{\partial z}\right]=0, \tag{1}$$

where p is the pressure divided by the density of the ambient fluid, ρ_a, and $\Delta=g(\rho-\rho_a)/\rho_a$. If we neglect the turbulent pressures, we may relate p at any height to its value at the roof p_r through the hydrostatic equation; so

$$p=p_r+\int_z^D \Delta\cos\alpha\,dz'. \tag{2}$$

We also have the continuity equation

$$\frac{\partial U}{\partial x}+\frac{\partial W}{\partial z}=0. \tag{3}$$

If we make use of these and integrate (1) from z to D, we obtain

$$\int_z^D\frac{\partial U^2}{\partial x}dz'-UW+(D-z)\frac{dp_r}{\partial x}+\frac{\partial}{\partial x}\int_z^D(z'-z)\Delta(z')\cos\alpha\,dz' + \int_z^D\Delta\sin\alpha\,dz'+(K_M+\nu)\frac{\partial U}{\partial z}=-\frac{\tau_r}{\rho_a}, \tag{4}$$

where τ_r is the stress at the roof. In the particular case when U and Δ are independent of x, this simplifies to

$$(M-z)\frac{dp_r}{dx}+\int_z^D\Delta\sin\alpha\,dz'+(K_M+\nu)\frac{\partial U}{\partial z}=0, \tag{5}$$

where M is defined by $(D-M)\,dp_r/dx=-\tau_r/\rho_a$.

The theoretical modification of velocity due to weight alone

We shall now use a simple theoretical model in which K_M is held fixed at its neutral value and approximated by a parabola to investigate how much the weight of the layer modifies the velocity profile. The density profile will be taken to have a triangular form, falling linearly with height from a surface value Δ_s to zero at a height h_A. This form is quite close to the observed density profile in all but very concentrated layers except in small regions near the floor and near h_A; since only an integral of the density profile enters the calculation, these regions may be neglected and it is not difficult to represent observed profiles by equivalent triangles.

Thus, our assumptions are

$$K_M = K_0 \frac{z}{D}\left(1-\frac{z}{D}\right); \tag{6}$$

$$\begin{aligned} \Delta &= \Delta_s\left(1-\frac{z}{h_A}\right) && \text{for } z \text{ less than } h_A, \\ &= 0 && \text{for } z \text{ greater than } h_A. \end{aligned} \tag{7}$$

We also assume that U is zero at the same distance z_0 from the roof and the floor, and that z_0 may be considered constant; we take $z_0/D = 2\times 10^{-4}$, which is the value appropriate to smooth flow at the Reynolds number of our experiments.

For convenience we introduce the following dimensionless variables:

$$\Pi = D^2 K_0^{-1} U_{\bar{d}}^{-1} dp_r/dx; \quad \mu = M/D; \quad \delta = D^2 K_0^{-1} U_{\bar{d}}^{-1} \Delta_s \sin\alpha;$$

$$\sigma = D^{-1} U_{\bar{d}}^{-1} \Delta_s^{-1} \int_0^D \Delta U\, dz; \quad \xi = h_A/D; \quad \zeta = z/D; \quad \upsilon = D U_{\bar{d}}^{-1} dU/dz;$$

where $U_d = D^{-1}\int_0^D U\,dz$. Then we see that the pipe Richardson number, which was introduced in the first part of this paper, is given by

$$\mathrm{Ri}_p = U_{\bar{d}}^{-3} \int_0^D \Delta U \cos\alpha\, dz = \sigma\delta K_0 D^{-1} U_{\bar{d}}^{-1} \cot\alpha.$$

If molecular viscosity is neglected, it follows from (5) that

$$\begin{aligned} \upsilon &= \frac{(\zeta-\mu)\,\Pi - \delta\xi[\tfrac{1}{2} - \xi^{-1}\zeta + \tfrac{1}{2}\xi^{-2}\zeta^2]}{\zeta(1-\zeta)} && \text{for} \quad \zeta \leqslant \xi, \\ &= \frac{(\zeta-\mu)\,\Pi}{\zeta(1-\zeta)} && \text{for} \quad \zeta > \xi. \end{aligned} \tag{8}$$

Hence after integration,

$$\begin{aligned} \frac{U}{U_d} &= \tfrac{1}{2}\xi^{-1}\zeta\delta - (\mu\Pi + \tfrac{1}{2}\delta\xi)\ln\zeta/\zeta_0 \\ &\qquad - [(1-\mu)\,\Pi + \delta(1-\tfrac{1}{2}\xi^{-1} - \tfrac{1}{2}\xi)]\ln(1-\zeta) \quad \text{for} \quad \zeta \leqslant \xi, \\ &= -\mu\Pi\ln\zeta - (1-\mu)\,\Pi\ln\frac{1-\zeta}{\zeta_0} \quad \text{for} \quad \zeta > \xi. \end{aligned} \tag{9}$$

μ and Π may now be found from the conditions that U is continuous at $\zeta = \xi$ and that $\int_0^1 \frac{U}{U_d} d\zeta = 1$. We obtain

$$\Pi = \frac{-2+\delta[-\frac{1}{2}+\frac{3}{2}\xi-\frac{1}{2}\xi\ln\xi/\zeta_0+(1-\frac{1}{2}\xi^{-1}-\frac{1}{2}\xi)\ln(1-\xi)]}{\ln\zeta_0^{-1}-2}, \tag{10}$$

and

$$(2\mu-1)\,\Pi = \frac{\delta[\frac{1}{2}-\frac{1}{2}\xi\ln\xi/\zeta_0-(1-\frac{1}{2}\xi^{-1}-\frac{1}{2}\xi)\ln(1-\xi)]}{\ln\zeta_0^{-1}}. \tag{11}$$

The dimensionless salt flux σ can be evaluated in an elementary manner using (7) and (9), and is given by

$$\begin{aligned}\sigma = {} & \mu\Pi[\tfrac{1}{2}-\tfrac{1}{2}\xi\ln\xi/\zeta_0-a\ln(1-\xi)] \\ & +\Pi[a\ln(1-\xi)-\tfrac{1}{2}+\tfrac{3}{4}\xi] \\ & +\delta[a^2\ln(1-\xi)-\tfrac{1}{4}\xi^2\ln\xi/\zeta_0+\tfrac{1}{4}\xi^{-1}+\tfrac{13}{12}\xi-\tfrac{7}{8}],\end{aligned} \tag{12}$$

where a has been written for $(1-\frac{1}{2}\xi-\frac{1}{2}\xi^{-1})$.

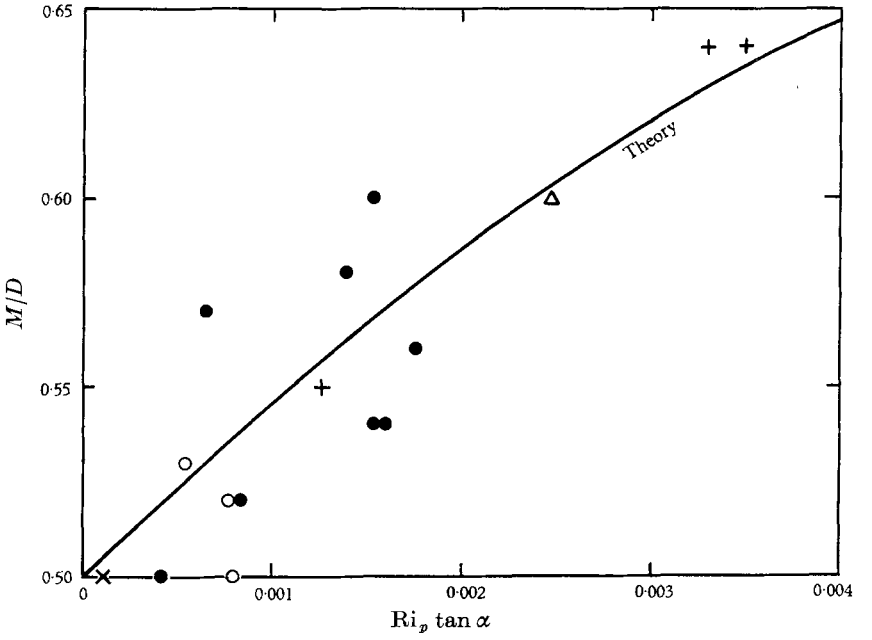

FIGURE 1. The height of the velocity maximum in an inclined pipe containing heavy salt solution as a function of $\mathrm{Ri}_p \tan\alpha$. The curve drawn is theoretical, and individual experimental points are shown. ○, 6°; +, 20°; ×, 7½°; △, 30°; ●, 10°.

With a knowledge of σ it is simple to calculate Ri_p. Since in each of our experiments Ri_p is independent of x it is convenient to make it the independent variable and to regard the profiles as functions of Ri_p and ξ. The dependence of μ on ξ for a fixed value of $\mathrm{Ri}_p \tan\alpha$ turns out to be so weak that μ can be represented adequately as a function of $\mathrm{Ri}_p \tan\alpha$ alone; this is plotted in figure 1 together with our observations of the height of the velocity maximum, which are further discussed below. Π also depends very little on ξ, and it is

clear that the distortion of the profile is much more closely governed by the channel Richardson number than by the depth of the layer, and we should not expect much change in velocity as the layer spreads. This provides some justification for the use of the simplified form of the equation of motion in which U and Δ are assumed to be independent of x. A comparison between a typical theoretical profile and observation will be discussed after the techniques of measurement have been described.

The measurement of velocity

Several methods were tried before consistent measurements of velocity were obtained. The low velocities made it impossible to use Pitot tubes, and at first an attempt was made to use thermistors as in an earlier investigation (Ellison & Turner 1959). They proved to be too inaccurate owing to the sensitivity of the system to ambient temperature, to the non-linearity of the calibration which caused difficulty in averaging the highly fluctuating velocity, and to the obstruction to the flow which became important when the thermistor was traversed more than half way across the pipe.

Later, a twisting wire device was tried, in which the deflexion of a fine steel wire set across the flow was observed with a microscope. This also failed to give the required accuracy, possibly because the drag of a cylinder depends on the level of turbulence in the stream.

The useful measurements were taken using the most direct method of all, that of timing streaks of dye released into the stream. Moveable opaque guides were placed on each side of the pipe so that they could be set at any given height and the motion of the dye along their open edge followed; the measurements were made between fixed marks drawn 30 cm apart at the positions of the salt probes. It was possible to time to the nearest $\frac{1}{20}$ sec in about 2 sec, and the variations greater than this were due to real variations in velocity from one realization of the flow to another; the average of ten readings was taken at each height and the standard deviation of this was about 3 %. In order to achieve this accuracy it was necessary to have an adequate length of pipe between the point of introduction of the dye and the first mark, so that the general appearance of the dye did not change appreciably between the stations. Systematic errors are likely to be small except near the roof or floor where the velocity gradient is high and one can unconsciously follow material at the wrong level.

Our estimates of the velocity gradients are, of course, much less accurate than those of velocity itself, and may be in error by 10 %; this means that our estimates of the local Richardson number may be out by 20 % due to the uncertainties of velocity alone.

We also attempted to measure velocity variations in the direction of flow by timing over overlapping intervals at the same height; we found that, except with very concentrated salt layers, the variations were less than the experimental errors in accordance with the theoretical prediction mentioned above.

The experiments were conducted using two standard discharge velocities, 13·5 and 10·6 cm s^{-1}, the majority being at the higher speed which is that used for the measurements reported in the first part of this paper.

Comparison with simple theory

Examples of measured velocity profiles are shown in figures 2 and 3. In figure 2 the experimental points (crosses) are compared with the theoretical curve calculated by the method outlined above; the measured density profiles and the 'equivalent triangle' assumed for the purpose of the calculation are also shown.

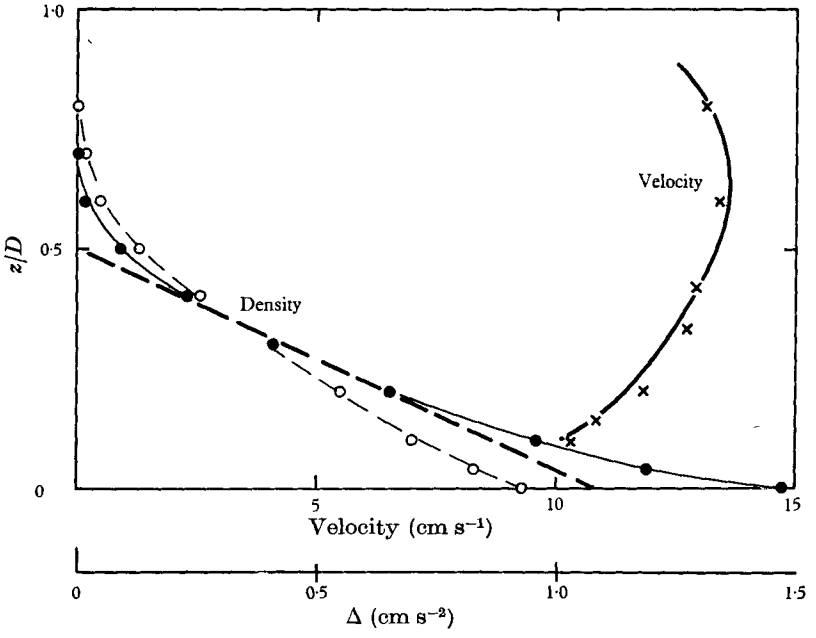

FIGURE 2. Comparison of observed and calculated velocity profiles in a pipe inclined at 20°; $\mathrm{Ri}_p = 0{\cdot}0090$. The density profiles 30 cm apart and the 'equivalent triangle' used in the calculation are also shown.

The general shape of the velocity profile is adequately represented by the theory, although the slopes of the theoretical curve are somewhat greater than those corresponding to the measured points in this instance. The height of the velocity maximum is well predicted; the more extensive measurements of this quantity shown in figure 1 also confirm that in spite of considerable scatter there is no systematic difference between the theory and the measurements. Thus it appears that the assumption that K_M is unchanged by the presence of the dense fluid is a fair first approximation and that the direct action of the weight of the layer is the most important factor distorting the velocity profile.

This suggests the possibility of using the theory in order to estimate the velocity gradients entering into the expression for the local Richardson number. For the determination of the dependence of K_S and K_M on Ri, we have preferred to use directly measured velocity profiles; but in §6 below we do develop an empirical extension of the theory in order to relate the eddy transport coefficients to the rate of increase of the depth of the layer described in detail in Part 1.

The theory is, of course, at its weakest when one considers thin concentrated layers at low slopes, since in these the effect of stability in reducing K_M is relatively more important.

3. The momentum transfer

From the measurements of velocity described in the last section and the density profiles obtained by the method described in Ellison & Turner (1959), it is possible to estimate the eddy viscosity K_M. The analysis was confined to occasions when the layer was not too thin and the velocity changed little in the x-direction. Then, since the only term in (4) depending on $\partial\Delta/\partial x$, namely

$$\frac{\partial}{\partial x}\int_z^D (z'-z)\,\Delta(z')\cos\alpha\,dz',$$

is quite negligible, it is permissible to use (5).

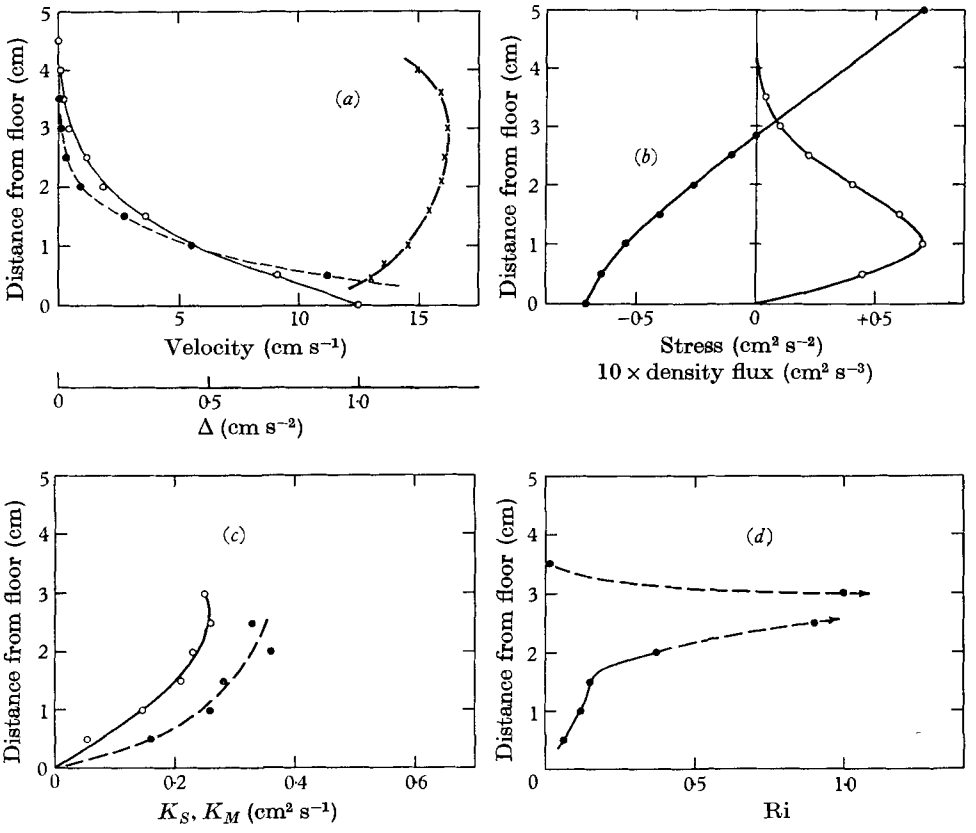

FIGURE 3. Turbulent transfer in a pipe inclined at 10°; $\mathrm{Ri}_p = 0{\cdot}0037$. (*a*) Measured velocity and density profiles. ●, Density at 40 cm; ○, density at 70 cm; ×, velocity. (*b*) Distributions of stress and density flux. ●, $-(K_M+\nu)\,dU/dz$; ○, $-K_S(d\Delta/dz)$. (*c*) Transfer coefficients for salt (K_S) and momentum (K_M). ●, K_M; ○, K_S. (*d*) Local Richardson number, Ri.

However, (5) contains two unknown quantities, dp_r/dx and M. In order to measure the pressure gradient directly a much more uniform pipe than ours would be required, even if the considerable difficulties of devising and using a sufficiently sensitive manometer could be overcome. We therefore had to make two assumptions to fix dp_r/dx and M:

(*a*) the friction coefficient relating the stress on the roof to the discharge velocity is the same as at the same Reynolds number without any salt flow;

(*b*) the total stress is zero at the height of the velocity maximum.

The first of these assumptions is unlikely to be far wrong, since there is never sufficient density gradient in the top half of the channel to give rise to any significant stability effects. The second assumption is not so satisfactory either theoretically or in practice. Although the idea behind the use of an eddy viscosity implies that the stress vanishes when the velocity gradient does, there is no theoretical reason for believing that this happens exactly; and in practice the measured velocity maxima are broad, making the determination of the position of no stress difficult and thus introducing another considerable source of error.

If these assumptions are accepted, K_M can be found from (5). However, reasonably consistent results could not be obtained either in the centre of the pipe where the velocity gradients are small and K_M is the ratio of two small quantities, or near the floor where the velocity gradients are too high to be determined by our technique. Our most accurate results are therefore restricted to the two heights 1·0 and 1·5 cm. Measurements at these positions have the additional advantage that usually the density flux and Richardson number are changing less rapidly with height in this region than elsewhere (see figures 3*b* and *d*).

In figures 3*a*, *b* and *c* are shown typical velocity and density profiles and the variation with height of the stress and eddy viscosity derived from them. We shall return to discuss the results of all the experiments analysed in this way after describing the calculation of the eddy diffusivity.

4. The salt transfer

In the steady state, with the neglect of turbulent transfer in the direction of the flow and of the minute contribution of molecular diffusion, the equation for the transfer of salt may be written

$$U\frac{\partial\Delta}{\partial x}+W\frac{\partial\Delta}{\partial z}-\frac{\partial}{\partial z}\left(K_S\frac{\partial\Delta}{\partial z}\right)=0. \tag{13}$$

When the velocity is independent of x, so that $W = 0$, this simplifies to

$$K_S\frac{\partial\Delta}{\partial z}=-\int_z^D U\frac{\partial\Delta}{\partial x}dz'. \tag{14}$$

The salt flux is zero at the top and bottom of the channel so the integral taken from 0 to D should be zero if U is in fact independent of x; and, in the absence of measurements of $\partial U/\partial x$ on every occasion, this has been used as a check in selecting runs for analysis. Values of the salt flux and of K_S calculated from (14) are included in figures 3*b*, and *c*.

5. The dependence of K_M and K_S on the local Richardson number

It is clear that K_M and K_S must depend on the stability, but since the scale of turbulence is such that any eddy covers a considerable height range, it is by no means obvious that there should be a simple dependence on a strictly local parameter such as

$$\mathrm{Ri}=-\frac{\partial\Delta}{\partial z}\Big/\left(\frac{\partial U}{\partial z}\right)^2$$

which changes with height as is shown for a typical occasion in figure 3*d*. Nevertheless, the curve obtained when the results are analysed in this way is very encouraging.

The eddy viscosity

The dependence of the eddy viscosity on the Richardson number has been discussed in the meteorological literature (see Charnock 1958 for a recent review). It is usual (Deacon 1955) to consider the dimensionless quantity $K_M^* = K_M/u_* z$,

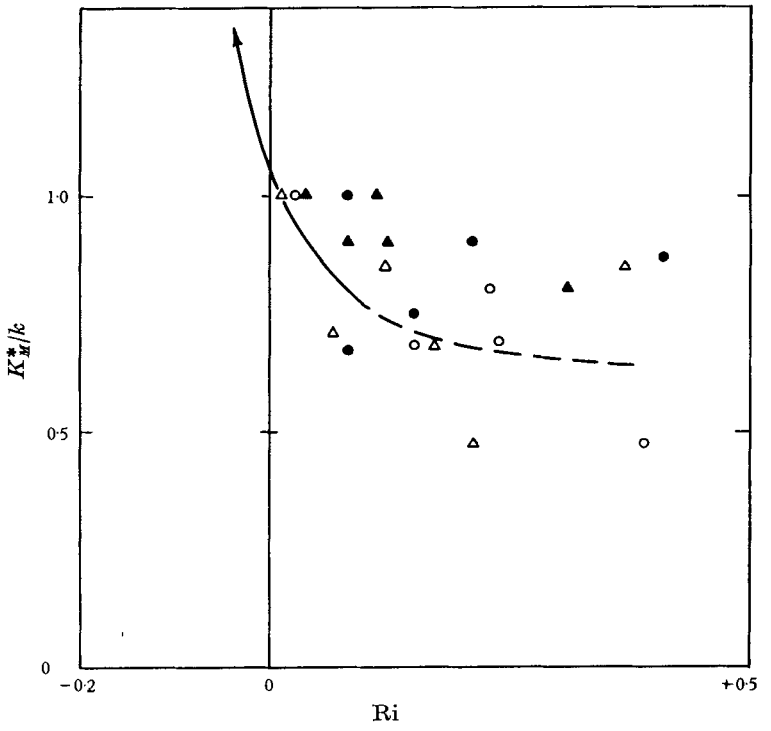

FIGURE 4. Measurements of the non-dimensional eddy viscosity K_M^*/k as a function of local Richardson number. ▲ △, 1·0 cm; ● ○, 1·5 cm. The curve drawn represents an average of the atmospheric measurements reported by Rider (1954).

where u_* is the friction velocity defined by $u_* = |K_M \partial U/\partial z|^{\frac{1}{2}}$. In figure 4 K_M^*/k, where k is von Karman's constant, is plotted as a function of Ri together with a curve which represents an average of Rider's (1954) widely scattered atmospheric measurements. Rider was mainly concerned with unstable conditions and took only a few measurements in the range of Richardson numbers for which we have dotted the curve.

Our measurements are also scattered, but they confirm the trend for K_M^* to fall below its neutral value, k, as Ri is increased. These results and those shown later for K_S have been grouped according to the accuracy with which $\int_0^D U \frac{\partial \Delta}{\partial x} dz'$ is zero. In the first group (indicated in the figures by solid symbols) are experiments for which the integral is zero to within the experimental accuracy; in the

second group (indicated by open symbols) are those for which the negative part of the integral at the bottom of the pipe is up to 50 % higher than the top part, indicating a small but probably negligible vertical velocity near the bottom of the pipe. Lastly, there are the experiments shown by crosses in some of the figures in which the criterion is clearly not satisfied. These correspond to cases when there was a very concentrated layer near the floor, and for which even from visual observation we should expect W to be important.

The ratio K_S/K_M

When we come to compare the ratio K_S to K_M, the scatter is less important since the dependence on Ri is more dramatic. In figure 5 are shown all the results at the two heights of 1·0 and 1·5 cm. The points for which significant values of W have been ignored lie low in the left-hand corner of the diagrams, which is to

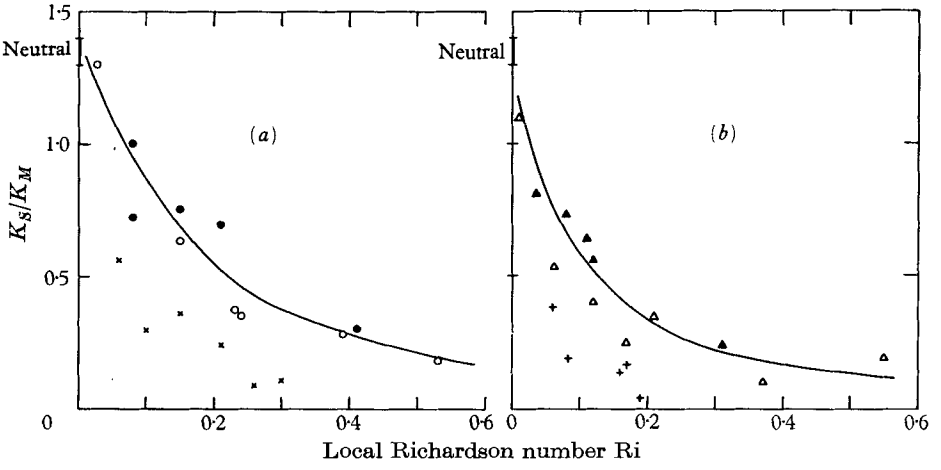

FIGURE 5. The ratio K_S/K_M as a function of the local Richardson number; (*a*) at 1·5 cm; (*b*) at 1·0 cm. The solid symbols refer to occasions when the vertical velocity was zero; the open symbols to occasions when it was measurable, but probably negligible, and the crosses to cases where a significant vertical velocity has been ignored.

be expected since neglect of W will increase the estimate of K_M and decrease that for K_S; the suggested 'best' curves have been drawn using only the more reliable points.

The difference between the results at the two levels are systematic but not very large; it is hard to say whether or not it is significant or on what factors, such as Reynolds number, it depends. The striking feature of the results is the sharp fall of K_S/K_M at quite small Ri, and this will now be discussed further in relation to previous measurements and theories.

Previous measurements of K_S/K_M

The possibility of a dependence of K_S/K_M on Ri has been discussed in the meteorological literature (e.g. Pasquill 1949; Rider 1954; Swinbank 1955), but the difficulties of measurement are great and accuracy has not been good, largely, we would suggest, because of the neglect of advection terms (cf. the neglect of

$\partial U/\partial x$ in our problem). A tendency for K_S/K_M to decrease with increasing Ri has been found, but there is not even agreement about the value of the ratio in neutral conditions: Rider gets 1·3 and Swinbank about 0·8.

Fortunately, there are more precise measurements in controlled laboratory conditions from which the neutral value can be found. Sherwood & Woertz (1939) made measurements in a nearly two-dimensional vertical duct one wall of which was covered with water and the other with strong calcium chloride solution, so that a humidity gradient was set up. They found that in the central region of the duct the eddy diffusivity for water vapour was around 1·5 times the eddy viscosity at a Reynolds number of 10^5.

Forstall & Shapiro (1950) measured profiles of velocity and helium concentration in a turbulent jet and also surveyed previous experimental results for the turbulent diffusion of heat (or matter) and momentum in both liquids and gases. They concluded that all the measurements led to a value for K_S/K_M within 10 % of 1·40.

In 1952 Page, Schlinger, Breaux & Sage reported an experiment in a small two-dimensional duct with the floor and roof maintained at different temperatures and through which air was flowing so rapidly in relation to the temperature gradients that Ri was negligible. They measured the ratio of the transfer coefficients as a function of position and Reynolds number, and found a value of 1·30 at the Reynolds number used in our pipe. Later Schlinger, Berry, Mason & Sage using the same apparatus gave a value appropriate to our case of 1·35 and suggested that it decreased to about 1·1 at very high Reynolds numbers. More recent reports from the same laboratory (Hsu, Sato & Sage 1956) disagree about the detailed dependence on Re, but this does not have much effect on the values we have taken. We can assert with some confidence that in neutral conditions and at the Reynolds number we used, K_S/K_M lies between 1·3 and 1·4; these limits have been marked in figures 5 and 6.

Our previous experimental results for wall plumes (Ellison & Turner 1959) can be reanalysed to give K_S and K_M. The calculation is tedious since W can certainly not be neglected and all the terms in the equations of motion must be determined, but we have carried it through for one case. At the height at which Ri was changing least and had a value of 0·23, we obtained $K_S/K_M = 0{\cdot}23$. This is not inconsistent with the present series of measurements and is marked with them on figure 6.

At the extreme of very high Richardson numbers, there are the frequently quoted measurements made in the Kattegat under conditions of very great stability, which have often been used to verify that the flux Richardson number, $\mathrm{Rf} = \mathrm{Ri}\,K_S/K_M$, is always less than unity. The analysis of Proudman (1953) shows that K_S/K_M is between 0·05 and 0·03 when Ri is in the range from 4 to 10. It is likely that the difference in Reynolds number between our experiments and the oceanographic observations is important; and, moreover, there is a strong probability that at very high Richardson numbers the transfer mechanism may be more closely associated with the breaking of internal waves than with turbulence in the ordinary sense (Stewart 1959). Nevertheless, Proudman's estimates are quite consistent with an extrapolation of our results and are shown together with them in figure 6.

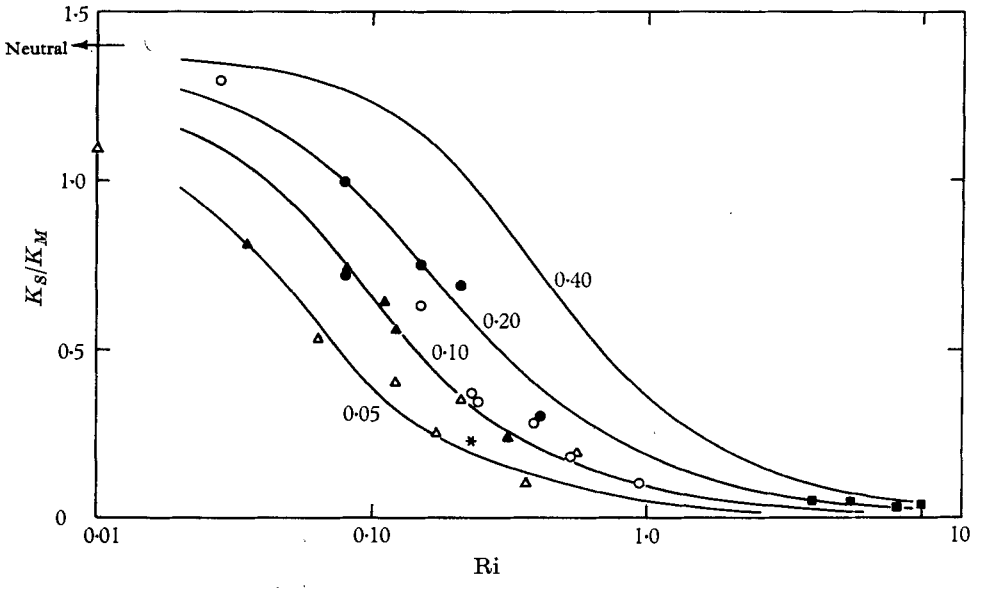

FIGURE 6. The comparison of our experimental results and other available data with the theory of Ellison (1957). The values of the parameter Rf_c are marked on the theoretical curves. ● ○, 1·5 cm; ▲ △, 1·0 cm; ⁎, Wall plume; ■, Kattegat.

Comparison with the theory of Ellison (1957)

In 1957 Ellison presented a speculative theory which predicts dependence of K_S/K_M on Ri. Using the equations of motion, continuity and diffusion together with some assumptions concerning the rates at which the velocity and density fluctuations and their covariance would decay in the absence of the terms in the equations describing their production, Ellison arrived at an equation (numbered 20 in his paper) of the form

$$\frac{K_S}{K_M} = \frac{b(1-\mathrm{Rf}/\mathrm{Rf}_c)}{(1-\mathrm{Rf})^2}, \tag{15}$$

where b and Rf_c are constants or very slowly varying functions which depend on the structure of the turbulence. Clearly b is the value of K_S/K_M in neutral conditions and Rf_c is the critical value of Rf at which K_S vanishes. In order to evaluate the constants, Ellison made further numerical assumptions, but we can do this directly from our experimental results. With K_S/K_M in neutral conditions fixed at 1·4, say, (15) gives a family of curves connecting K_S/K_M to Rf (or Ri) with Rf_c as parameter, and these are drawn in figure 6. Our results at 1·5 cm are seen to be fitted best by the curve corresponding to $\mathrm{Rf}_c = 0{\cdot}15$, but if we include our measurements at 1·0 cm, the best estimate of Rf_c will be nearer to 0·10.

Note that even at higher Ri the theoretical curves are broadly in agreement with the Kattegat measurements. In this range, however, the assumption that b and Rf_c are constants independent of stability is less likely to be accurate, and in any case the comparison between theory and experiment is less reliable in this range. By using the range where K_S/K_M depends strongly on stability, we have obtained a more sensitive comparison with theory.

Ellison's original estimate for Rf_c was 0·15, and our results are in surprisingly close agreement with this, confirming his conclusion that Rf_c is much less than unity. This is a remarkable result, since it implies that the term representing the rate of working against buoyancy forces in the turbulent energy equation, which is commonly invoked at the beginning of discussions of turbulence in a stratified fluid, is never dominant; the rate of transfer of dense fluid is drastically affected before the direct effects of the reduction of turbulent energy could make themselves felt. Further clues about the operative mechanism may be obtained from Ellison's paper. The expression for the correlation coefficient between density and vertical velocity given by him leads to

$$\frac{(\overline{w'\Delta'})^2}{\overline{w'^2}\,\overline{\Delta'^2}} \propto \frac{1-\mathrm{Rf}/\mathrm{Rf}_c}{1-\mathrm{Rf}}. \tag{16}$$

Thus as Rf approaches Rf_c the correlation between velocity and density is destroyed more rapidly than the fluctuations themselves. This suggests the simple physical picture that in stable conditions a displaced fluid particle tends to return to its equilibrium level before it has mixed with its surroundings. A particle can transfer momentum during a brief excursion without mixing, but in order to transfer matter or heat it must mix.

6. Conclusions

The work we have described in this paper forms an intermediate link in the chain of knowledge leading from the detailed equations of motion to the magnitudes of the spread of salt solution, the measurements of which were recorded in Part 1. On the one side it is connected to the theory, as yet very imperfect, relating the transfer coefficients to the local Richardson number as has been described in §5; and it must be possible to link it on the other side with some calculation of the development of the density profiles yielding values of dh/dx from those of K_S and K_M. We shall outline such a calculation in an appendix.

We may now summarize our main conclusions as follows:

(1) In tilted pipes the weight of the dense fluid is the dominant factor modifying the velocity profile; the changes in K_M due to stability and to the alteration in the stress distribution are less important.

(2) Our results are consistent with, but do not establish, a reduction of K_M^* with increasing Richardson number of the magnitude suggested by the meteorological observations.

(3) Our measurements show that K_S/K_M is strongly dependent on the Richardson number. The form found for this dependence (figures 5 and 6) is likely to have wide validity, but the numerical values may be in error by 30–50 %. It must also be stressed that strictly they apply only to one particular region in the pipe and may be affected somewhat by the shape of the pipe and the Reynolds number.

The investigation described was made in the course of work carried out for the Ministry of Power on problems relating to the movement of firedamp in the roadways of coal mines. One of us (J.S.T.) wishes to acknowledge the financial support of the Ministry of Power.

REFERENCES

CHARNOCK, H. 1958 *Sci. Progr.* **46**, 470–87.

DEACON, E. L. 1955 *Comm. Sci. Ind. Res. Org., Div. Met. Phys.* (*Melbourne*), *Tech. Pap.* no. 4.

ELLISON, T. H. 1957 *J. Fluid Mech.* **2**, 456–66.

ELLISON, T. H. & TURNER, J. S. 1959 *J. Fluid Mech.* **6**, 423–48.

ELLISON, T. H. & TURNER, J. S. 1960 *J. Fluid Mech.* **8**, 514–28.

FORSTALL, W. & SHAPIRO, A. H. 1950 *J. Appl. Mech.* **17**, 399–407.

HSU, N. T., KAZUHIKO SATO & SAGE, B. H. 1956 *Industr. Engng Chem.* **48**, 2219–23.

PAGE, F., SCHLINGER, W. G., BREAUX, D. K. & SAGE, B. H. 1952 *Industr. Engng Chem.* **44**, 424–30.

PASQUILL, F. 1949 *Proc. Roy. Soc.* A, **198**, 116–40.

PROUDMAN, J. 1953 *Dynamical Oceanography*. London: Methuen.

RIDER, N. E. 1954. *Phil. Trans.* A, **246**, 481–501.

SCHLINGER, W. G., BERRY, V. J., MASON, J. L. & SAGE, B. H. 1953 *Industr. Engng Chem.* **45**, 662–6.

SHERWOOD, T. K. & WOERTZ, B. B. 1939 *Trans. Amer. Inst. Chem. Engrs*, **35**, 517–40.

STEWART, R. W. 1959 *Advances in Geophysics*, Vol. 6, *Proceedings of Symposium on Atmospheric Diffusion and Air Pollution* (Oxford, August 1958), pp. 303–10. New York and London: Academic Press.

SWINBANK, W. C. 1955 *Comm. Sci. Ind. Res. Org., Div. Met. Phys.* (*Melbourne*), *Tech. Pap.* no. 2.

Appendix

The relation between the measurements of K_S/K_M and dh/dx

If we had shown that K_M^* and K_S/K_M were everywhere exactly determined by the local value of Ri and had found the form of the dependence, a complete set of equations would be available and in principle it would be possible to start with an arbitrary distribution of concentration and calculate its development; but our measurements were much too limited for that. In any case, such a calculation would be highly complex and we must beware of doing elaborate calculations on the basis of inadequate information. Nevertheless, it seems desirable to make some attempt to relate our new knowledge of the transfer coefficients to the rate of spread of the layer, and we shall therefore present a brief description of a very crude semi-empirical approach to the problem, which doubtless can be refined as understanding increases.

For this purpose we shall again use the simple model proposed in §2 in which the density profile is assumed to be triangular. Although this form is adequate for calculating the distortion of the velocity profile, the actual density profiles do depart considerably from it in some circumstances, especially near $z = h$. We have tried several more elaborate models which take this into account, but the improvement in accuracy is only moderate, and we have chosen to present only the simplest here.

It is convenient to divide the calculation into stages as follows.

(*a*) The determination of the local Ri at a standard height, which we have chosen to be $\frac{1}{2}\xi$, as a function of Ri_p, ξ, and α.

(*b*) The use of our empirical relation between K_S/K_M and Ri, together with the assumption that K_M is given by (6), to obtain K_S at the height $\frac{1}{2}\xi$ as a function of Ri_p, ξ, and α.

(*c*) The relation of K_S to $\partial\xi/\partial x$ at this height.

(*d*) The relation of h to ξ and so the determination of dh/dx as a function of Ri_p, ξ, and α.

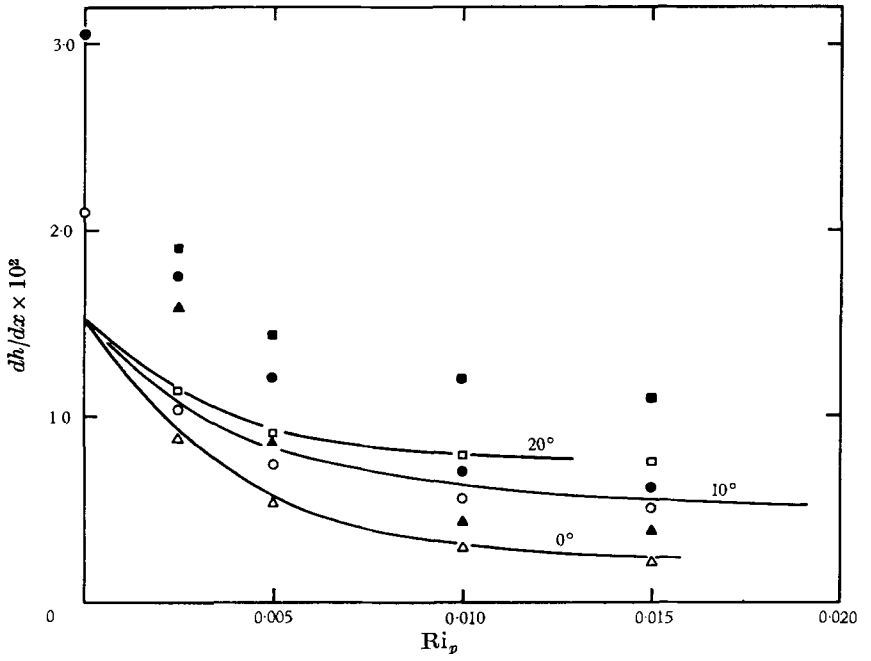

FIGURE 7. Theoretical estimates of the rate of spread of the layer using experimental values of K_S/K_M. The curves represent the measured values of this quantity which were reported in Part 1.

	$\xi = 0{\cdot}4$	$\xi = 0{\cdot}6$
0°	▲	△
10°	●	○
20°	■	□

The first stage is simple since it follows from the definitions in §2 that $\mathrm{Ri} = \sigma^{-1}\xi^{-1}\upsilon^{-1}\mathrm{Ri}_p$; σ and υ are known functions of ξ and δ (for $\zeta = \frac{1}{2}\xi$) and δ depends on ξ and $\mathrm{Ri}_p \tan\alpha$. This means that $\mathrm{Ri}\tan\alpha$ is a function of $\mathrm{Ri}_p \tan\alpha$ and ξ. The numerical dependence has been computed for two values of ξ, 0·4 and 0·6, because for these $\frac{1}{2}\xi$ corresponds to the two heights 1·0 and 1·5 cm at which we measured K_S/K_M. It is found that in both cases $\mathrm{Ri}\tan\alpha$ is proportional to $\mathrm{Ri}_p \tan\alpha$ when the quantities are small, but changes only slowly when $\mathrm{Ri}_p \tan\alpha$ is large. This explains an effect which proved troublesome during our experiments: it was impossible to obtain large local Richardson numbers except at small slopes.

The second stage of the calculation follows quite directly. For the third stage we use equation (14) and assume that we may replace U in it by U_d. Then, since Δ is given by (7),

$$\frac{K_S\Delta_s}{U_d h_A} = \frac{h_A}{8}\frac{d\Delta_s}{dx} + \tfrac{3}{8}\Delta_s\frac{dh_A}{dx} = \frac{\Delta_s}{8}\left[\frac{h_A}{\Delta_s}\left(\frac{\partial\Delta_s}{\partial h_A}\right)_{\mathrm{Ri}_p} + 3\right]\frac{dh_A}{dx}. \tag{17}$$

Now, the numerical value of $h_A \Delta_s^{-1} (\partial \Delta_s / \partial h_A)_{\mathrm{Ri}_p}$ varies little with $\mathrm{Ri}_p \tan \alpha$ and ξ and is around $-1{\cdot}2$, so

$$\frac{K_S}{U_d h_A} = 0{\cdot}22 \frac{dh_A}{dx}. \tag{18}$$

This equation and equation (6) gives K_S/K_M.

For the last stage it is necessary only to observe that, by definition, $\sigma = \Delta_d/\Delta_s$, and so

$$h = h_A(1-\sigma). \tag{19}$$

The final results are shown in figure 7. The points represent the theoretical values of dh/dx as a function of Ri_p for the slopes 0°, 10° and 20°, at the two values of ξ 0·4 and 0·6, corresponding roughly to $h = 1{\cdot}7$ cm. and 2·2 cm, and they are compared with our earlier experimental curves given in Part 1. It will be seen that this semi-empirical theory explains the general shape of the curves and the dependence on slope, and shows clearly the range of pipe Richardson number where stability becomes important. It is, however, less good at small values of Ri_p and predicts a dependence of dh/dx on ζ which was not observed (but which may, of course, be detected in more refined experiments). In view of the very crude approximations that were made and the experimental difficulties at small Ri_p, these discrepancies are not surprising and the qualitative success of the theory suggests that further progress will be made as increasing experimental information enables it to be refined.